Changes in Independency between Two Types of El Niño Events under a Greenhouse Warming Scenario in CMIP5 Models

YOO-GEUN HAM AND YERIM JEONG

Faculty of Earth Systems and Environmental Sciences, Chonnam National University, Gwangju, South Korea

JONG-SEONG KUG

School of Environmental Science and Engineering, Pohang University of Science and Technology (POSTECH), Pohang, South Korea

(Manuscript received 20 October 2014, in final form 17 June 2015)

ABSTRACT

This study uses archives from phase 5 of the Coupled Model Intercomparison Project (CMIP5) to investigate changes in independency between two types of El Niño events caused by greenhouse warming. In the observations, the independency between cold tongue (CT) and warm pool (WP) El Niño events is distinctively increased in recent decades. The simulated changes in independency between the two types of El Niño events according to the CMIP5 models are quite diverse, although the observed features are simulated to some extent in several climate models. It is found that the climatological change after global warming is an essential factor in determining the changes in independency between the two types of El Niño events. For example, the independency between these events is increased after global warming when the climatological precipitation is increased mainly over the equatorial central Pacific. This climatological precipitation increase extends convective response to the east, particularly for CT El Niño events, which leads to greater differences in the spatial pattern between the two types of El Niño events to increase the El Niño independency. On the contrary, in models with decreased independency between the two types of El Niño events after global warming, climatological precipitation is increased mostly over the western Pacific. This confines the atmospheric response to the western Pacific in both El Niño events; therefore, the similarity between them is increased after global warming. In addition to the changes in the climatological state after global warming, a possible connection of the changes in the El Niño independency with the historical mean state is discussed in this paper.

1. Introduction

Based on recent advances in the understanding of the El Niño–Southern Oscillation (ENSO) phenomenon, many aspects of the mechanisms of ENSO modulation due to increasing anthropogenic forcing have been investigated (van Oldenborgh et al. 2005; Philip and van Oldenborgh 2006; An et al. 2008; Collins et al. 2010; Vecchi and Wittenberg 2010; Watanabe et al. 2012; Spencer and Braswell 2014). Collins et al. (2010) used a simple theoretical interpretation of global climate change in the weakening of the mean atmospheric overturning circulation (Held and Soden 2006; Vecchi et al. 2006) to report the changes in oceanic and atmospheric feedbacks related to the El Niño genesis based on the mean state change under the global warming scenario. They argued that several atmospheric and oceanic feedbacks related to ENSO are amplified and some are weakened after global warming, which explains the diverse changes in amplitude by the climate model simulation of ENSO. For example, two important oceanic ENSO feedbacks, thermocline feedback and zonal advective feedback (Jin and An 1999), would be enhanced after global warming. However, atmospheric damping of the ENSO-related sea surface temperature (SST) anomaly is also expected to increase under the global warming scenario.

In addition, several studies have emphasized the role of the spatial pattern of ENSO-related atmospheric response in the changes in ENSO variability after global

Corresponding author address: Prof. Jong-Seong Kug, School of Environmental Science and Engineering, Pohang University of Science and Technology (POSTECH), 77 cheongam-Ro Nam-Gu, Pohang 790-784, South Korea.
E-mail: jskug1@gmail.com

DOI: 10.1175/JCLI-D-14-00721.1

warming (An et al. 2008; Kug et al. 2010a; Collins et al. 2010; Seiki et al. 2011). Kug et al. (2010a) showed that in most coupled general circulation models (CGCMs) in phase 3 of the Coupled Model Intercomparison Project (CMIP3) archives, tropical Pacific warming due to an increase in CO_2 concentration promotes ENSO-related convection centers in the equatorial Pacific to the east, which may amplify the ENSO amplitude (Kang and Kug 2002; Kim et al. 2008, 2011; An et al. 2008; Watanabe et al. 2012). Power et al. (2013) also showed that this eastward shift in the convection center during ENSO is quite robust in most of the climate models and global warming scenarios, although huge diversity occurs in changes in the ENSO amplitude after the global warming. In addition, Seiki et al. (2011) showed that ENSO-related high-frequency atmospheric variability is increased over the eastern Pacific under global warming because the eastward-extended warm pool can facilitate the development of organized convection over the eastern Pacific.

In addition to the possible changes in the overall amplitude of ENSO, it has recently been argued that the frequency of extreme El Niño events can be increased by global warming (Cai et al. 2014; Johnson 2014; Min et al. 2015). Cai et al. (2014) estimated the changes by aggregating the results of climate models in the CMIP3 and phase 5 of CMIP (CMIP5; IPCC 2014) multimodel databases and a perturbed physics ensemble. They showed that increased frequency of El Niño events with extreme amplitudes is caused by projected surface warming over the eastern equatorial Pacific that occurs faster than that in the surrounding ocean waters, which facilitates more occurrences of atmospheric convection in the eastern equatorial region. Johnson (2014) argued that this increased frequency in extreme El Niño events is robust even if the model results fail to achieve a consensus on the changes in overall ENSO amplitude after global warming.

In addition, increasing attention has been given to the frequency of different types of El Niño modes, which include date line El Niño (Larkin and Harrison 2005a,b), El Niño Modoki (Ashok et al. 2007), central Pacific (CP) El Niño (Kao and Yu 2009), and warm pool (WP) El Niño (Kug et al. 2009; Kug and Ham 2011); these types can change in the warm climate (Ashok and Yamagata 2009; Yeh et al. 2009, 2014; Lee and McPhaden 2010; Takahashi et al. 2011). Lee and McPhaden (2010) mentioned that the intensity of CP El Niño has almost doubled during the past three decades, with the strongest warming occurring in 2009/10. In addition, Yeh et al. (2009) showed that CP El Niño has occurred more frequently during the recent decades and that such changes are also prominent in the global warming scenarios of CMIP3. They suspected that the change in oceanic basic state after global warming is responsible for this increasing frequency of CP El Niño. That is, the shallow thermocline over the central Pacific can enhance the central Pacific SST variability. However, cautious perspectives maintain the difficulty in such conclusions because the recent increasing frequency of CP El Niño is indistinguishable from natural variability (Newman et al. 2011; Yeh et al. 2011; Johnson 2013; Taschetto et al. 2014).

Although most previous studies have focused on the changes in the frequency of two types of El Niño events, few reports have examined whether El Niño after greenhouse warming can be successfully distinguished as two types. Of course, the increased frequency of WP El Niño can be related to independency between two types of El Niño events to some extent, particularly in the observations, because cold tongue (CT) El Niño has been dominant in previous decades. However, the main interest of the independency between the two types of El Niño events is different from the arguments about the frequency. The former is based on whether the ENSO characteristics would be increased after global warming, and the latter is based on whether the warmer climate is favorable for El Niño duality or diversity. In addition, the increased frequency of the WP El Niño events is not closely linked to independency between the two types of El Niño events in climate models, which will be discussed in more detail in the final section of this paper.

On the basis of such motivations, this study examines the changes in independency of the two types of El Niño events after greenhouse warming by using the latest CMIP archives (i.e., CMIP5), which implies that the global warming signal can lead to greater distinction in the two types of the El Niño events. In addition to the multimodel ensemble (MME) response, we investigate the responses of the individual models in the causes of differences in independency between the two types of events among climate models. Second, we show a possible role of atmospheric responses during El Niño in the changes in independency between two types of El Niño events after global warming. This paper is organized as follows. Section 2 describes the CMIP5 archives and observational data. Section 3 covers the changes in independency between the two types of El Niño events and explores the possible reasons under the global warming scenario. A summary and discussion is given in section 4.

2. Model and data

We analyzed 36 climate models integrated with a maximum 156 years of the historical scenario and a maximum 95 years of the representative concentration pathway 4.5 (RCP4.5) scenario in the CMIP5 archives. The linear

TABLE 1. Description of models obtained from the CMIP5 archives. (Expansions of acronyms are available online at http://www.ametsoc.org/PubsAcronymList.)

Model No.	Modeling group	CMIP ID	Historical run integration		RCP4.5 integration period	
			Period (yr)	No. of ensemble members	Period (yr)	No. of ensemble members
1	NASA GISS	GISS-E2-H	156	15	95	14
2	NOAA/GFDL	GFDL CM3	146	1	95	1
3	CMCC	CMCC-CMS	156	1	95	1
4	IPSL	IPSL-CM5B-LR	156	1	95	1
5	NASA GISS	GISS-E2-H-CC	156	1	95	1
6	NASA GISS	GISS-E2-R	156	21	95	16
7	CCSR–JAMSTEC	MIROC-ESM-CHEM	156	1	95	1
8	NSF–DOE–NCAR	CESM1(CAM5)	156	3	95	3
9	NASA GISS	GISS-E2-R-CC	156	1	95	1
10	CCSR–JAMSTEC	MIROC5	156	5	95	3
11	National Institute for Meteorological Research/Korean Meteorological Administration (NIMR/KMA)	HadGEM2-AO	146	1	94	1
12	BCC	BCC_CSM1.1(m)	156	3	95	1
13	CCSR–JAMSTEC	MIROC-ESM	156	3	95	1
14	CSIRO	CSIRO Mk3.6.0	156	10	95	10
15	Met Office Hadley Centre	HadCM3	146	10	30	10
16	MRI	MRI-CGCM3	156	5	95	1
17	BCCR	BCC_CSM1.1	156	3	95	1
18	IPSL	IPSL-CM5A-LR	156	4	95	4
19	BNU	BNU-ESM	156	1	95	1
20	Météo-France	CNRM-CM5	156	1	95	1
21	CCCma	CanESM2	156	5	95	5
22	Met Office Hadley Centre	HadGEM2-ES	146	4	95	4
23	Norwegian Climate Centre (NCC)	NorESM1-ME	156	1	95	1
24	NOAA/GFDL	GFDL-ESM2G	145	3	95	1
25	MPI for Meterology (MPI-M)	MPI-ESM-LR	156	3	95	3
26	IPSL	IPSL-CM5A-MR	156	1	95	1
27	NOAA/GFDL	GFDL-ESM2M	145	1	95	1
28	CCCma	CanCM4	45	10	30	10
29	MPI-M	MPI-ESM-MR	156	3	95	3
30	NSF–DOE–NCAR	CESM1(BGC)	156	1	95	1
31	Met Office Hadley Centre	HadGEM2-CC	146	1	94	1
32	NCC	NorESM1-M	156	3	95	1
33	CMCC	CMCC-CM	156	1	95	1
34	CCSR–JAMSTEC	MIROC4h	56	3	30	3
35	NCAR	CCSM4	156	6	95	6
36	INM	INM-CM4.0	156	1	95	1

trend is removed before analyzing the data in both scenarios. Model references, details on the institutions in which the models were run, and integration periods are summarized in Table 1. For comparison with the model results, we used the monthly-mean SST data. The observed SST data include the improved Extended Reconstructed Sea Surface Temperature version 3b (ERSST V.3b) from the National Climate Data Center (Smith et al. 2008). This data analysis uses 2° spatial resolution "superobservations," which are defined as individual observations averaged onto a 2° grid. The SST period was 64 years from 1950 to 2013 during December–February (DJF).

3. Changes in two types of El Niño events under global warming scenario

To investigate the models' fidelity in simulating the two types of El Niño events, we first define the CT and WP El Niño events as reported by Kug et al. (2009). The Niño-3 [SST anomaly (SSTA) over 5°S–5°N, 150°–90°W] and Niño-4 (SSTA over 5°S–5°N, 160°E–150°W) indices are used for defining CT and WP El Niño, respectively. CT El Niño events occur when the Niño-3 index during the DJF season is greater than one standard deviation and the Niño-4 index. Similarly, WP El Niño is defined

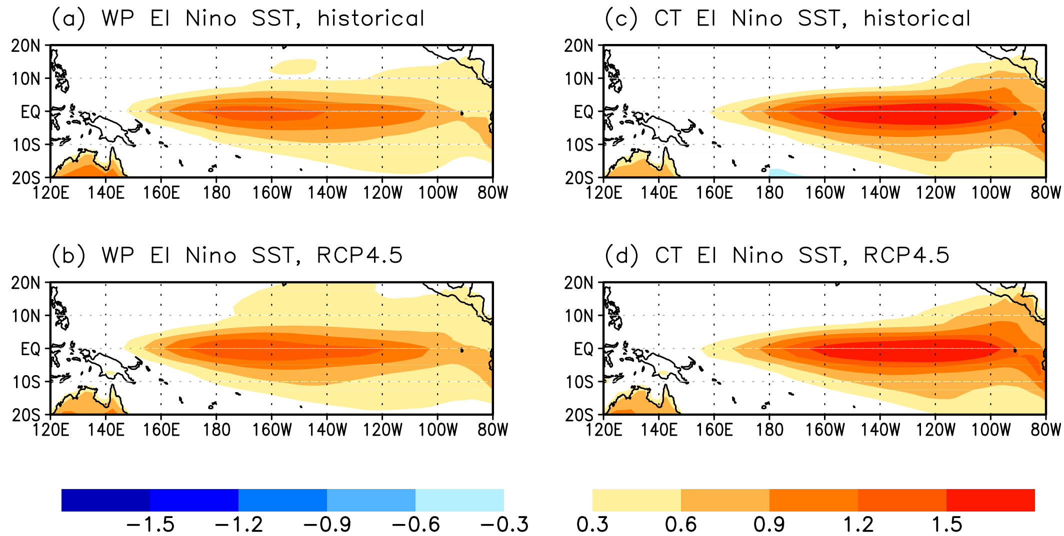

FIG. 1. MME DJF SSTAs (°C) during (a) WP El Niño in the historical run, (b) WP El Niño in the RCP4.5 scenario, (c) CT El Niño in the historical run, and (d) CT El Niño in the RCP4.5 scenario.

by using SST anomalies during the DJF season when the Niño-4 index is greater than one standard deviation and the Niño-3 index. According to this definition, Fig. 1 shows the MME DJF SSTAs during CT and WP El Niño in the historical run and RCP4.5 scenario. For the WP El Niño, the CMIP5 model results in the historical run shows the SSTAs shifted too far toward the western Pacific compared to the observed (Kug et al. 2012). For the CT El Niño, the models tend to simulate a stronger central Pacific SSTA than that observed. About the change in the spatial pattern after the global warming, the difference in spatial pattern of CT and WP El Niño after global warming is not clear in the MME. Similarly, the spatial pattern of CT El Niño is quite similar in both scenarios. These results imply that there may be no clear difference in independency between the two types of El Niño events, at least in the MME.

Figure 2 is the same as Fig. 1, but for precipitation anomalies. The amplitude of precipitation anomalies is slightly stronger in the RCP4.5 scenario in both El Niño events (Kug et al. 2012), and the precipitation anomalies during the CT El Niño are shifted slightly to the east in the RCP4.5 scenario (Power et al. 2013). However, similar to the ENSO-related SSTAs, precipitation anomalies do not show systematic changes in the spatial pattern of El Niño events after greenhouse warming. This result

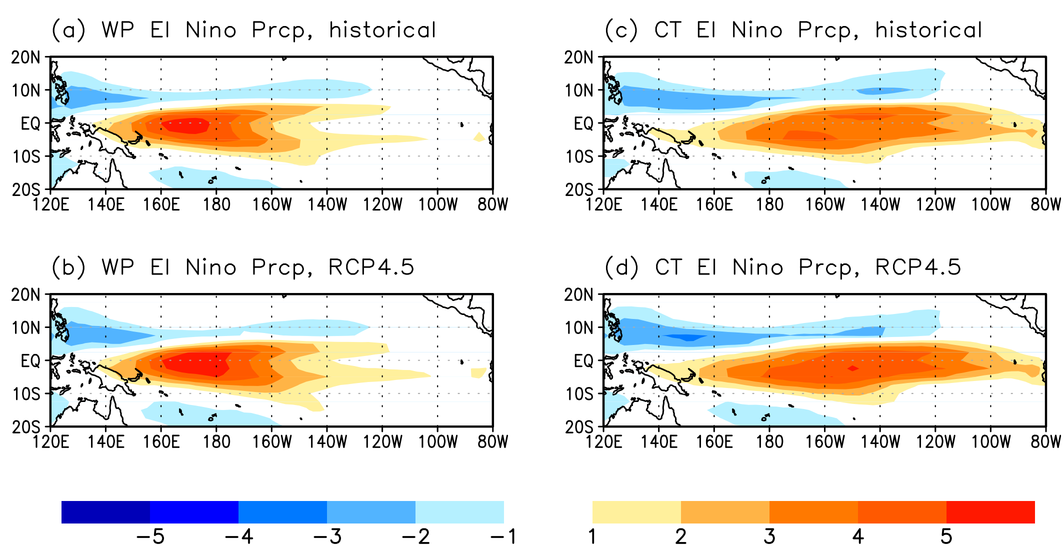

FIG. 2. As in Fig. 1, but for precipitation anomalies (mm day^{-1}).

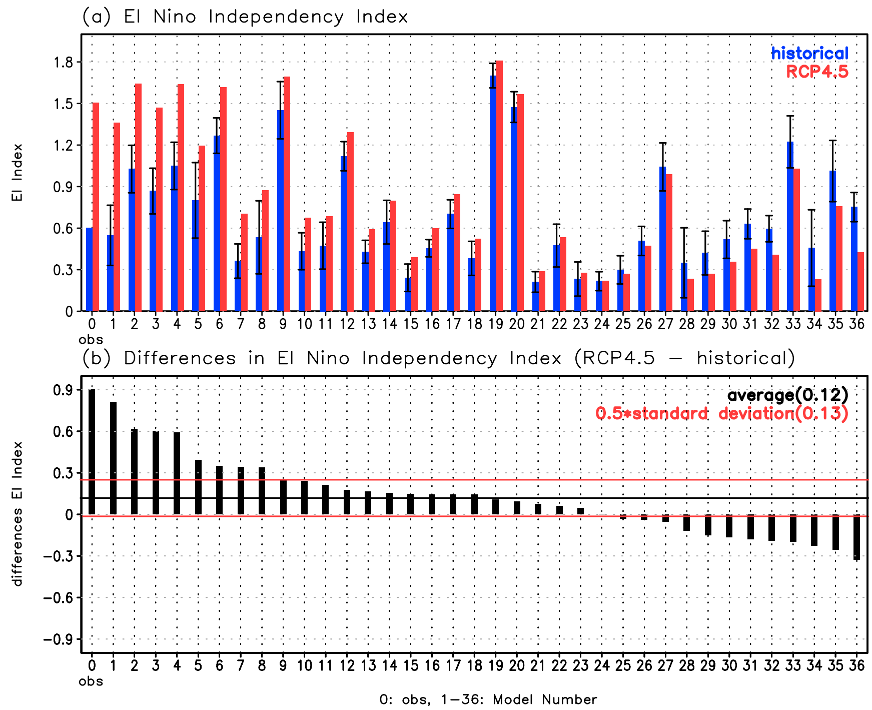

FIG. 3. (a) EI index calculated from the correlation coefficient between DJF Niño-3 and DJF Niño-4 SSTAs in the historical run (blue) and the RCP4.5 scenario (red). The error bar in the historical scenario denotes the 95% confidence level for the difference in the EI index using the bootstrap method. (b) Difference in EI index in the historical run from that in the RCP4.5 scenario. The red line denotes a 0.5 standard deviation from the average of differences. The number 0 on the *x* axis in (a) denotes the observed EI index during 1950–79 (blue) and 1980–2013 (red), and numbers from 1 to 36 represent each model.

implies that the MME does not show clear changes in independency between the two types of El Niño events.

Although no clear changes are apparent in the spatial pattern of El Niño events in the MME, however, significant changes are detected in the spatial pattern and independency between the two types of El Niño events in individual climate models. Thus, we focus on the responses of individual models rather than the MME result. Through this analysis, we expect to understand the crucial factors for determining the changes in ENSO characteristics after greenhouse warming. Moreover, the individual responses prevent overconfidence presented by the MME result, which is insensitive to global warming.

For analyzing each model's response, we need to quantify the degree of the independency between the two types of El Niño events. For this purpose, we first calculate the correlation coefficient between DJF Niño-3 and DJF Niño-4 SSTAs in historical and RCP4.5 scenarios. It should be noted that the correlation is calculated for only El Niño events reported by Ham and Kug (2012); thus, this correlation tends to be far smaller than the correlation using the entire period. The high correlation denotes that the simulated El Niño was mostly a single type, whereas the negative correlation denotes the model simulated two types of El Niño events independently. Note that, if the model has an extremely weak variability over Niño-4 region, the El Niño independency (EI) index for the model can be low even though the model has single type of El Niño event. However, we check that the Niño-4 variability is comparable to Niño-3 variability in all CMIP5 models to some extent (i.e., not smaller than 50% of Niño-3 variability), so this case (i.e., low EI index in the model with single type of El Niño) is not likely to happen, at least in our analysis. Because the independency is increased as the correlation between Niño-3 and Niño-4 is decreased, we subtract those correlation values from 1 (i.e., 1 − cor); this value is determined to be the EI index. Figure 3 shows the EI index in the two different decades in the observations (i.e., from 1950 to 1979 and from 1980 to 2013), and the historical and RCP4.5 scenarios in CMIP5 archives. The error bar in the historical scenario denotes the 95% confidence level based on the bootstrap method to examine whether the difference in the EI index in CMIP5 models is significant. For the significance test, we randomly select the same number of cases to that in the

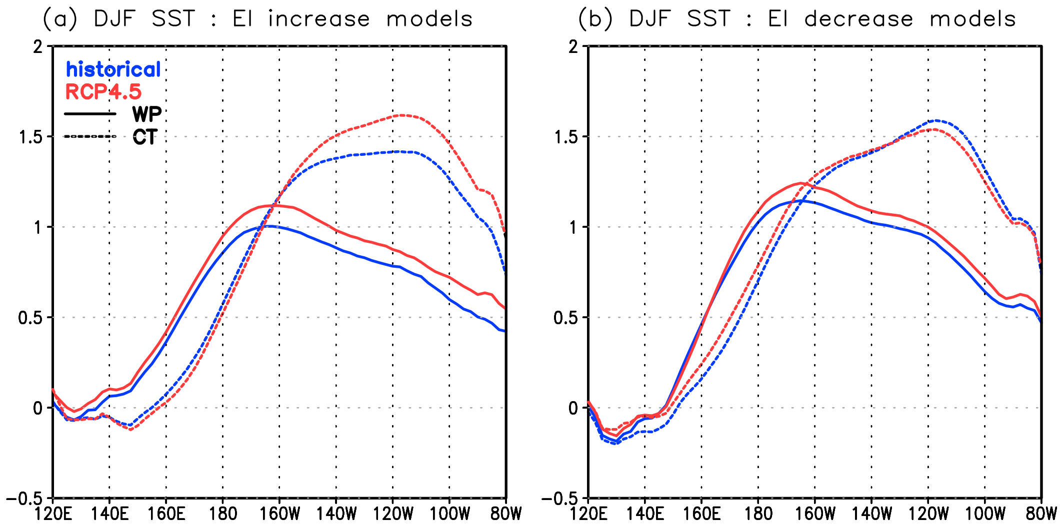

FIG. 4. Equatorially (5°S–5°N) averaged DJF SSTAs (°C) for the composite of WP El Niño (solid line) and CT El Niño (dashed line) in the (a) EI increase models and (b) EI decrease models in the historical run (blue) and the RCP4.5 scenario (red).

RCP4.5 scenario among historical simulations and then repeat this procedure 1000 times. For example, in the case of single ensemble member, among total 156 DJF cases in the historical simulation, 95 DJF cases (i.e., number of samples in RCP4.5 scenario) are randomly selected 1000 times. Then, the EI index is calculated for 1000 sets of samples, and then the standard deviation of the EI index from 1000 sets is calculated. Finally, a two-tailed Student's t test is performed using this standard deviation of the EI index.

In the observations, the EI index in previous decades (i.e., from 1950 to 1979) is 0.59, whereas that in recent decades (i.e., from 1980 to 2013) is distinctively increased to 1.45. These results are consistent with the increasing independency between the two types of El Niño events in recent decades (Yeh et al. 2009; Lee and McPhaden 2010). This observed feature is simulated in some climate models to some extent. Among 36 models, 24 show an increased EI index in the RCP4.5 scenario over that in the historical run. In addition, the EI index is slightly increased after global warming (i.e., the mean difference in EI index in the historical run from that in RCP4.5 is 0.12). These results indicate that the two types of El Niño events exhibit distinction after global warming in those climate models. On the contrary, the EI index is decreased in response to the global warming in 11 models, indicating a huge intermodel diversity in the model responses.

To investigate this intermodel diversity in greater detail, we categorize several climate models into two groups. The first is EI increase models, in which the EI index is increased significantly more than 0.5 standard deviations from the historical to RCP4.5 scenarios (models 1–8). The second is EI decrease models, in which the EI index is reduced significantly more than −0.5 standard deviations from the historical to RCP4.5 scenarios (models 25–36). Most of the models either in the EI increase or EI decrease groups show that the change in the EI index after global warming is significant at 95% confidence level. We add this discussion and figure in a revised manuscript. By comparing the differences in the two groups, we examine the most important factors in determining the changes in independency between the two types of El Niño events after greenhouse warming.

To examine the relationship between the changes in the EI index and that in the spatial pattern of the El Niño events, Fig. 4 illustrates the DJF SST composite of WP and CT El Niño in both scenarios. In the EI increase models, the spatial pattern between WP and CT El Niño is likely to differ greatly in the RCP4.5 scenario as the SST signal of the CT El Niño is weakened over the eastern Pacific, and slightly weakened over the central Pacific. On the other hand, in the EI decrease models, the positive SST anomalies in the CT El Niño signal become weaker over the eastern Pacific and slightly stronger in the central Pacific in the RCP4.5 scenario, which reduces the difference between the two types. This shows that the similarity in spatial patterns between two types of El Niño events can be measured by the EI index to some extent. That is, the decrease (increase) in EI index after global warming denotes that the similarity in the spatial patterns between the two types of El Niño events is increased (decreased).

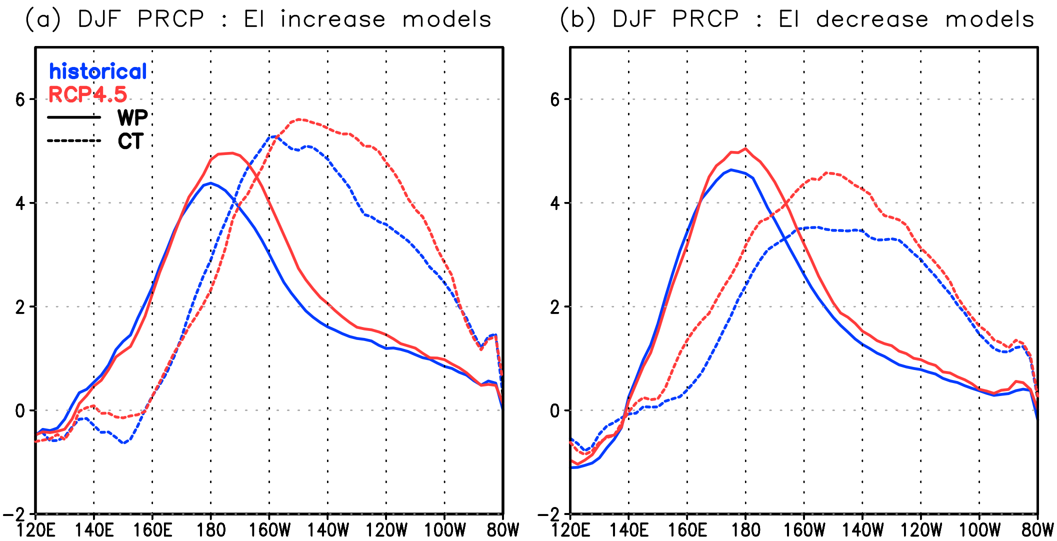

FIG. 5. As in Fig. 4, but for precipitation anomalies (mm day^{-1}).

Such changes in the spatial patterns of WP and CT El Niño between the two scenarios are consistent in the DJF precipitation composite, as shown in Fig. 5. In the EI increase models, the peak locations of the positive precipitation anomaly during both El Niño events are clearly extended to the east after the warming. Between WP and CT El Niño events, this extension after global warming is wider for the CT El Niño events, which leads to the greater difference between the two types of El Niño events after global warming. In the EI decrease models, however, the similarity between the two types of El Niño events is likely to be increased in the RCP4.5 scenario. There is a slight zonal extension of the WP El Niño precipitation to the east after the global warming, whereas the CT El Niño composite shows the increase of precipitation mainly over the western-central Pacific after the global warming. For example, the precipitation increase during the CT El Niño after the global warming is not clear to the east of 120°W, while there is increase in precipitation response between 140°E and 120°W. The pattern correlation between the WP and CT El Niño precipitation composite is increased from 0.68 in the historical run to 0.76 in the RCP4.5 scenario. Therefore, the similarity in the spatial pattern between the two types of El Niño events is increased in the RCP4.5 scenario.

Interestingly, it appears that the changes in the CT El Niño pattern are key in determining the similarities between the spatial patterns of the two types of El Niño events and therefore the independency between these events. That is, although the change in the spatial distribution of WP El Niño is relatively close between two EI groups, the extension of CT El Niño–related convection anomalies to the east (west) were critical for increasing (decreasing) the independency between the two types of El Niño events (i.e., the EI index). It is also worthwhile to note that the precipitation responses of the CT El Niño are weaker in the EI decrease models than those in the EI increase models, although the magnitude of the SST anomaly is slightly stronger. It shows that the atmospheric responses of the EI decrease models are less sensitive to the eastern Pacific SST forcings. These differences may be important for determining future changes in El Niño independency.

We then attempt to determine controlling factors in EI index diversity among climate models. This diversity can be related to the changes in the basic states of models. To verify this, Fig. 6 shows the changes in climatological precipitation in the RCP4.5 simulation from that in the historical run in the MME. Also, the differences in climatological precipitation changes in EI increase models and EI decrease models are shown by subtracting the MME in order to examine the differences in climatological change in the two groups. For the significance test, we perform a Student's t test using the standard deviation based on each model's deviation from the MME. In the MME, the climatological precipitation is increased mostly over the equatorial Pacific, which is consistent with that reported in previous studies (Allen and Ingram 2002; Watanabe et al. 2014). In particular, climatological precipitation shows a robust increase over the central Pacific and a weak decrease over the off-equatorial eastern Pacific. In the EI increase models, the difference is positive over the equatorial central Pacific, indicating that the climatological precipitation is further increased over the equatorial central Pacific than that in the MME. On the contrary, decreases

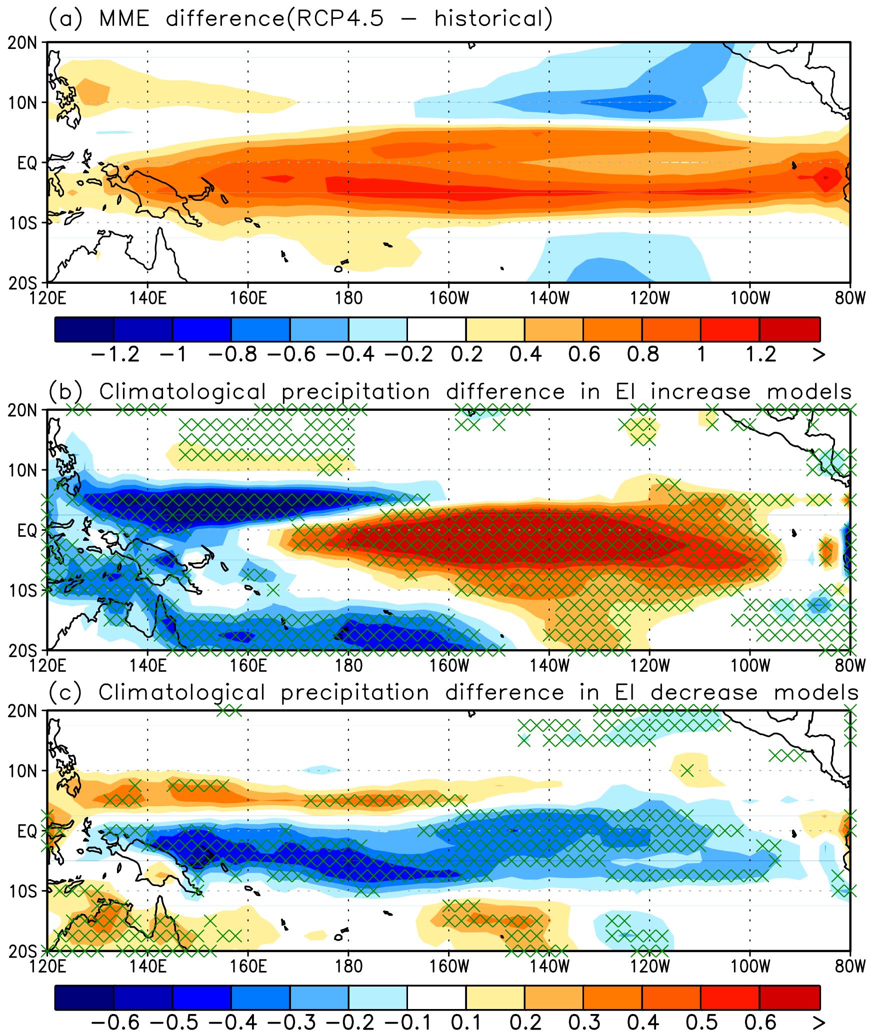

FIG. 6. (a) MME difference in climatological precipitation (mm day^{-1}) in RCP4.5 simulation from that in the historical run. (b) Deviation of the climatological precipitation difference in the EI increase models from that in the MME. (c) As in (b), but for EI decrease models. Green crosses denote a 95% statistical confidence level based on a Student's t test.

in climatological precipitation are found over the off-equatorial western Pacific. This indicates that the zonal gradient of the precipitation over the Pacific is weakened, implying a more weakened Walker circulation. The EI decrease models show opposite signals, in which the climatological precipitation is increased significantly over the equatorial western Pacific. In addition, the increase in climatological precipitation over the equatorial central Pacific is clearly less than that in the MME. In short, the climatological precipitation in the RCP4.5 scenario is enhanced and extended to the east in the EI increase models and confined over the western Pacific in the EI decrease models.

One can wonder whether the changes in the ENSO can cause the changes in the mean precipitation by rectifying the ENSO signal (Kessler and Kleeman 2000; Watanabe and Wittenberg 2012; Ham et al. 2012). Recently, Watanabe and Wittenberg (2012) developed a methodology that can separate the impact of the mean precipitation changes due to the changes in ENSO probability distribution (i.e., changes in ENSO amplitude/asymmetry). By adopting their study, we calculate the correlation between the mean precipitation change over the Niño-3 region with and without removing the impact of ENSO probability distribution change. It is found that two indices exhibit strong correlation (i.e., 0.77), implying that the change in the ENSO probability distribution is not responsible for change in the mean precipitation change, consistent with the results in Watanabe and Wittenberg (2012).

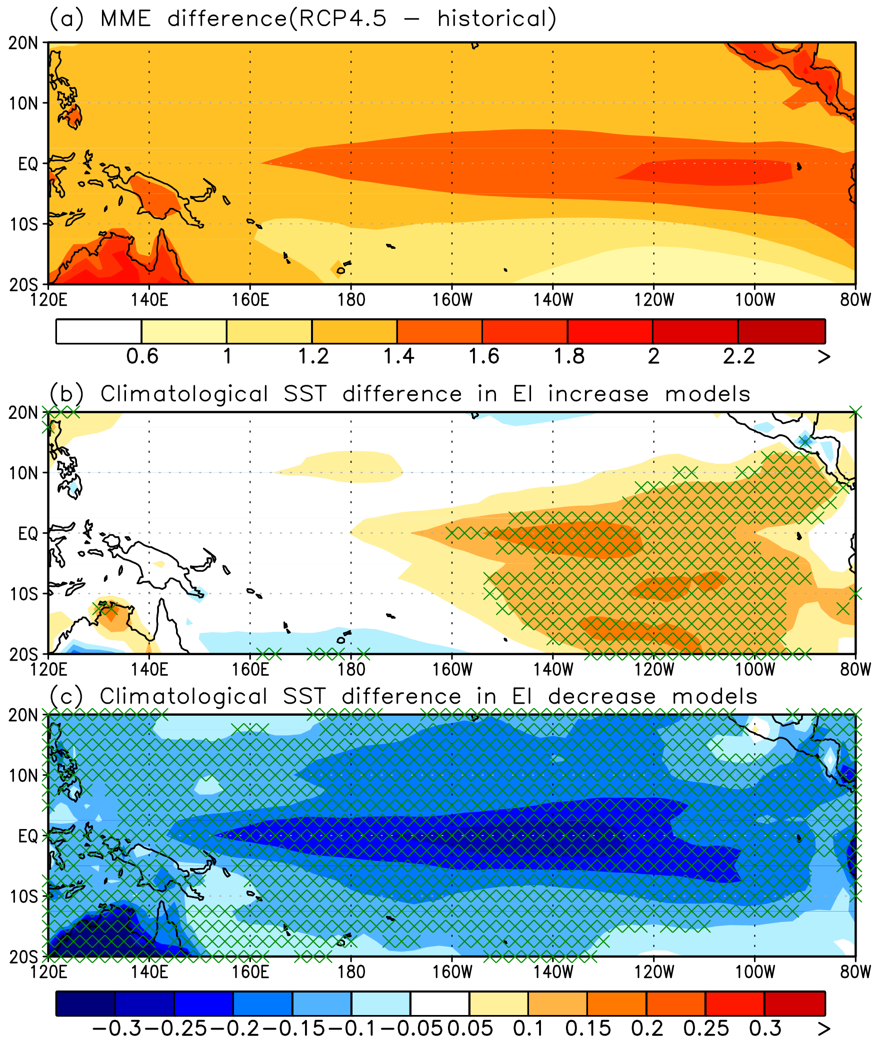

FIG. 7. As in Fig. 6, but for SSTAs (°C).

These changes in precipitation climatology are dynamically linked to those at the oceanic surface. Figure 7 shows the changes in climatological SST between the RCP4.5 simulation and the historical run, and the differences in the changes in climatology in the EI increase and decrease models. In the MME, robust warming in SST occurred over the equatorial central-eastern Pacific that resembled an El Niño–like pattern (Collins et al. 2005; Kug et al. 2011; An et al. 2012). In the EI increase models, in which the precipitation increase is enhanced over the central Pacific, SST warming is stronger over the central-eastern Pacific than that in the MME, which also enhances the MME SST change. These SST changes would have weakened the zonal SST gradient, leading to an eastward extension of climatological precipitation to the central-eastern Pacific (Kim et al. 2011). Conversely, the SST warming over the central Pacific in the EI decrease models is slightly weaker than that in the MME. These results are dynamically consistent with a smaller increase in precipitation over the equatorial central-eastern Pacific in the EI decrease models.

To examine this relationship between the climatology change and independency between the two types of El Niño events (i.e., EI index) in all CMIP5 archives, Fig. 8 shows a scatter diagram of changes in the mean precipitation over the eastern Pacific (i.e., 10°S–10°N, 140°–110°W) and that in the EI index using the 36 CMIP5 models. A strong positive relationship is clear between changes in the EI index and those of climatological precipitation over the eastern Pacific, which is consistent with the composite analysis. This implies that the relationship shown in Fig. 6, particularly the difference in the EI index and that in climatological precipitation after global warming, is also valid for the entire CMIP5 archive. The correlation coefficient between them is 0.66. This significant positive correlation denotes that

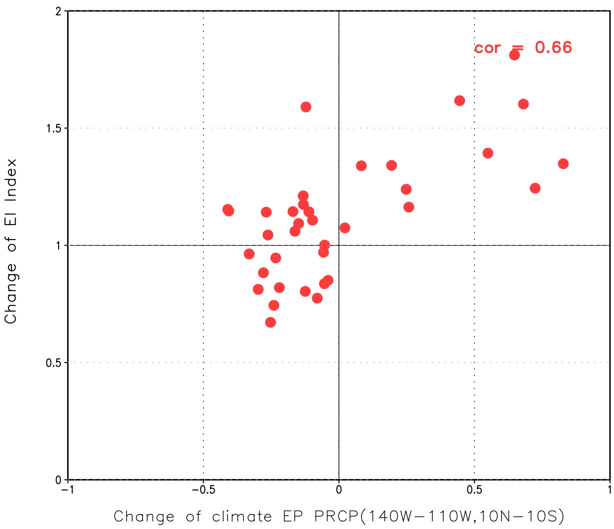

FIG. 8. Scatterplot showing changes in climatological precipitation over the eastern Pacific (i.e., 10°S–10°N, 140°–110°W) and that in the EI index using 36 CMIP5 models.

the models in which the precipitation increase is greater over the eastern Pacific tend to have two independent types of El Niño events after global warming, whereas those in which the precipitation increase over the central-eastern Pacific is weaker tend to show a reduction in independency between the two types after global warming.

We then examine how the changes in climatology over the tropical Pacific lead to changes in independency between the two types of El Niño events. Ham and Kug (2012) reported that climate models with drier climatology over the eastern Pacific than that in other models tend to simulate single types of El Niño events because such dryness results in anomalous El Niño–related convective activity confined over the western Pacific regardless of the location of the SST forcing. This leads to a similar atmospheric response between CT and WP El Niño, which is related to the low EI index (i.e., low independency between the two types of El Niño events). However, anomalous convective activity over the eastern Pacific can be generated during CT El Niño with the aid of wet local climatology; the atmospheric response during this type can differ from that during WP El Niño, in which the convective activity is confined to the western Pacific. Therefore, two types of El Niño can be simulated.

Their argument can be applied to the relationship between the changes in the climatology and that in the EI index between the historical run and the RCP4.5 scenario. The EI index can be increased such that two types of El Niño events become independent after global warming, when the climatological precipitation over the eastern Pacific is increased significantly to allow the ENSO-related convection response over the eastern Pacific during CT El Niño events. The convection response during the WP El Niño is also shifted to the east. However, that movement is not as clear as the eastward shift of convection during CT El Niño because the SST forcing during WP El Niño is confined over the central Pacific, which leads to larger zonal phase differences between the WP and CT El Niño events. Conversely, the models with decreased EI index tend to have smaller precipitation increases over the central Pacific to confine the atmospheric response during CT El Niño to the western Pacific. This westward shift in precipitation response leads to a response similar to that during WP El Niño, which increases the coupling between the two types of El Niño events.

To verify this hypothesis, we investigate the convection response to the SST anomalies with various zonal locations. The equatorial SST indices are defined for different longitude domains covering 60 longitudes from 150°E to 120°W with a 10° interval. For example, the indices for the centers at 150° and 160°E are area-averaged over 5°S–5°N, 120°–180°E and 5°S–5°N, 130°E–170°W, respectively. Then, after calculating the regressed precipitation anomalies with respect to each SST index, we calculate a centroid of the regressed precipitation pattern, defined as follows:

$$\text{PRCP Centroid} = \frac{\displaystyle\int \text{PRCP}(x)x\,dx}{\displaystyle\int \text{PRCP}(x)\,dx},$$

where PRCP(x) denotes the precipitation anomalies averaged over 5°S–5°N, and x denotes the longitude. The centroid of the PRCP anomaly is supposed to estimate the longitudinal center of the positive precipitation anomaly to the specified SSTA forcing. The zonal integration is executed over 120°E–90°W. This definition was used by Kug et al. (2010b).

Figure 9 shows the longitudinal center of precipitation response to the longitudinally varying SST indices in EI increase and decrease models. The zonal location of convective response naturally migrates eastward when the SST indices move to the east. The EI increase models show changes in precipitation location that are much more sensitive to the different locations of SST forcing in the RCP4.5 scenario than that in the historical run. For example, in the historical run, the zonal location of the precipitation center is located at 175°W when the SST forcing center is at 160°E, and it moves to around 165°W when the SST forcing center moves to 120°W. On the contrary, in the RCP4.5 scenario, when the SST forcing center is at 160°E, the precipitation center is located at around 180°, and it moves to 155°W when the

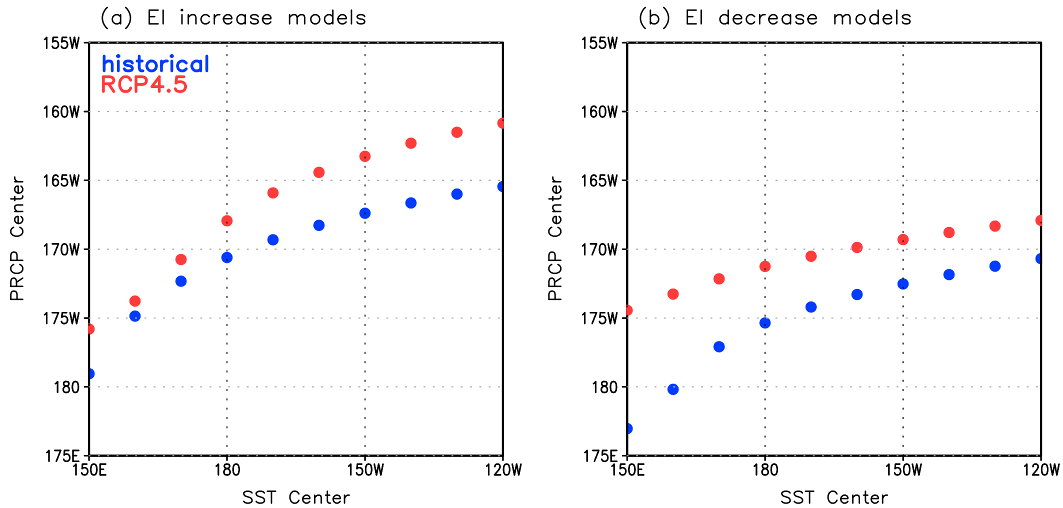

FIG. 9. Longitudinal center of precipitation response (mm day^{-1}) to longitudinally varying SST indices in the (a) EI increase and (b) EI decrease models. Blue and red dots denote the historical run and RCP4.5 scenario, respectively.

SST forcing center is at 120°W. These results show that the differences in the precipitation response between WP and CT El Niño would be larger in RCP4.5 scenario in EI increase models, which is consistent with the larger zonal phase difference of the precipitation composite shown in Fig. 5. In the EI decrease models, however, the differences in precipitation response to the different locations of SST forcing are clear in the historical run especially over the equatorial western Pacific. Although the precipitation response shifts gradually to 15° east when the SST forcing moved from 150°E to 120°W in the historical run, the precipitation response only moved less than 10° in the RCP4.5 scenario. This result clearly shows that sensitive precipitation response is important in independently simulating the two types of El Niño events.

In the models with an increased EI index after greenhouse warming, the variation of Niño-3 becomes independent from that of Niño-4 after the warming. This result is consistent with the fact that differences in the spatial patterns of WP and CT El Niño are greater in the RCP4.5 scenario. The climatological precipitation in those models increased mainly over the central-eastern Pacific in the RCP4.5 scenario, which leads to an eastward extension of the convective activity in both El Niño events. As this eastward extension of the convective response is greater during CT El Niño than that during WP El Niño, it leads to the two independent types of El Niño events. This occurs because the zonal phase difference between the SST forcing and precipitation response is greater in the CT El Niño events due to the weakened climatological dryness over the eastern Pacific in the RCP4.5 scenario. However, as it is more difficult for the convective response to extend farther east than the location of SST forcing, the convective activity remains over the western-central Pacific in WP El Niño even when the climatological dryness is weakened. On the contrary, the increase in climatological precipitation over the western Pacific is associated with the westward shift of the convective anomalies during CT El Niño, which leads to the decreased EI index.

Thus far, we have discussed the relationship between the changes in climatology and ENSO independency after global warming. In addition, we detected indications that the change in ENSO independency is also related to the historical mean state to some extent. Figure 10 shows the differences in climatological precipitation and SST bias in the historical run between the EI increase and EI decrease models. The differences in SST exhibit positive signals over the equatorial eastern Pacific, and the local precipitation climatology over the eastern Pacific is wetter in the EI increase models. These results imply that the models with warmer and wetter climatological states in the historical run can increase the EI index in the RCP4.5 scenario. As most of the climate models tend to have drier climatology with colder SST over the equator in the historical run than that in the observations (Lin 2007; Ham and Kug 2014), the positive SST and precipitation signal in historical climatology in the EI increase models tend to have realistic climatology in the historical run. That is, the models with realistic climatology in the historical run tended to simulate realistic changes in independency between the two types of El Niño events.

We then examine the reasons for which the historical mean state leads to changes in the EI index in the RCP4.5 scenario. The most probable possibility is based

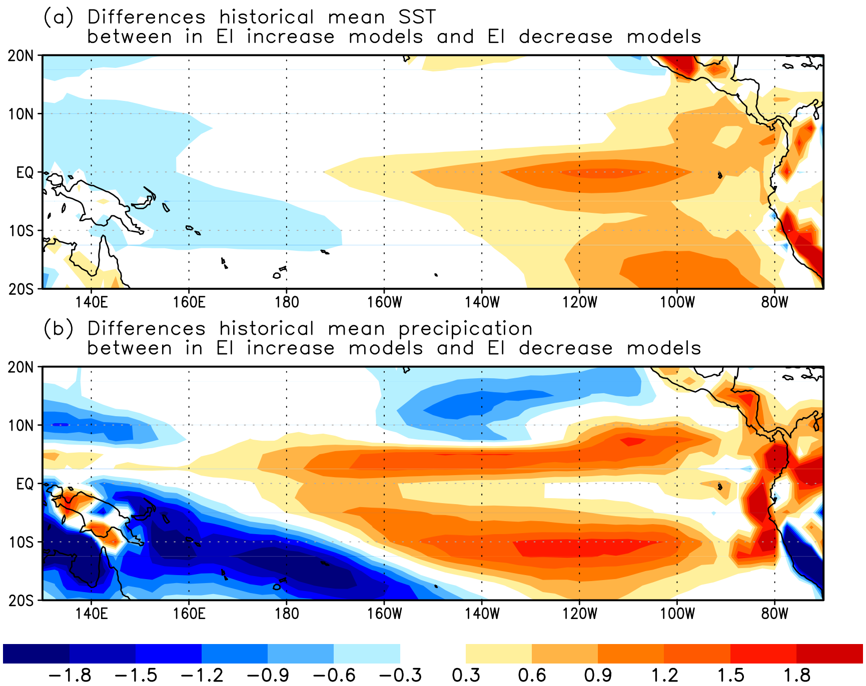

FIG. 10. (a) Differences between the historical mean SST in EI increase models and EI decrease models (EI increase model − EI decrease model). (b) As in (a), but for climatological precipitation (mm day^{-1}).

on previous studies about the robust relationship between historical wetness and the changes in wetness after global warming, known as the "wet gets wetter" mechanism (Held and Soden 2006; Chou et al. 2009). Once the climatology over the eastern Pacific is wetter and warmer, it allows the anomalous convection to amplify the climate change signal with relative ease. That is, SST warming due to the increased anthropogenic forcing can lead to significant changes in convective activity in models with wetter and warmer historical climatology, which in turn can lead to stronger Bjerknes feedback to strengthen the climate change signal (i.e., climate sensitivity). Therefore, the EI increase models tend to have wetter and warmer climatology in the historical run, which could have led to greater signals in wetness climate change after global warming over the equatorial eastern Pacific, in turn leading to an increase in independency between the two types of El Niño events. In addition, An et al. (2012) mentioned the role of the upwelling damping in climate sensitivity over the eastern Pacific. The warmer eastern Pacific could have caused the weaker low-level easterly, which would have weakened the upwelling amplitude, thereby also weakening the upwelling damping. According to this theory, the SST increase after global warming would be amplified in models with warmer historical mean states, therefore having a greater precipitation increase over the eastern Pacific. Then, it would allow ENSO-related convective activity to be shifted to the east to increase the independency between CT and WP El Niño (i.e., the EI index increases).

4. Discussion and summary

In this study, we used CMIP5 archives to investigate the changes in independency between two types of El Niño events due to global warming. In the observations, the independency between CT and WP El Niño events increased, which produced an increase in the EI index, for recent decades (i.e., from 1980 to 2013) compared with that in previous decades (i.e., from 1950 to 1979). The simulated changes in the EI index are quite diverse among the climate models even though this observed feature is simulated in some climate models.

It is shown that the change in simulated climatology after global warming is an essential factor in determining the changes in independency between the two types of El Niño events. The EI index is increased when the climatological precipitation is increased significantly over the equatorial central Pacific after global warming. The increase in climatological precipitation over the central Pacific extends the convective response to the east during both El Niño events; this feature is robust during CT El Niño. In models with decreased EI index

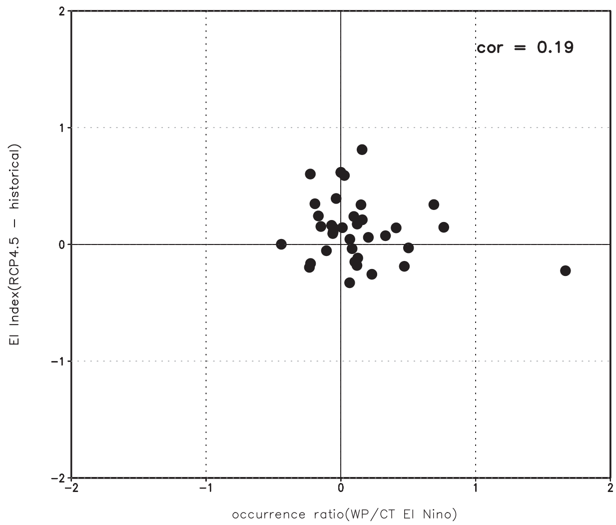

FIG. 11. Scatterplot showing differences in occurrence frequency ratio of WP El Niño to CT El Niño and that in the EI index in the RCP4.5 scenario and the historical run.

after global warming, however, climatological precipitation is increased significantly over the western Pacific and to a lesser degree over the central Pacific. This confines the atmospheric response to the western Pacific in both El Niño events; therefore, the similarity between them is increased after global warming.

As most previous studies have focused on whether the occurrence frequency of WP El Niño events would be increased after global warming (Yeh et al. 2009; Lee and McPhaden 2010), we examine the linkage between the change in occurrence frequency of WP El Niño and that in independency of the two types. In the observations, WP El Niño frequently occurred in recent decades, and the independency of the two types of El Niño events appeared to have increased. Therefore, it appears that the increase in frequency of WP El Niño is related to the increase in independency between the two types of El Niño events in the observations. However, the increase in frequency of WP El Niño events is not always linked to weakening of the coupling between the two types. Figure 11 shows a scatter diagram illustrating the differences in the occurrence frequency ratio of WP El Niño to CT El Niño and the EI index. It should be noted that the calculation procedure for the occurrence ratio is the same as that used by Yeh et al. (2009). No clear relationship is detected between the two indices. The correlation between them is 0.15, which implies that other factors have roles in controlling the two indices. It is determined that although the occurrence ratio is mostly dependent on the amplitude or spatial pattern of WP El Niño only, the EI index is also dependent on the CT El Niño pattern (not shown). This occurs because the EI index is used mainly to measure independency between the two types of El Niño events; therefore, changes in CT El Niño also can change the EI index. Conversely, the occurrence ratio is used mainly to measure the signal related to WP El Niño only. As global warming influences WP El Niño and CT El Niño, the linkage between the occurrence ratio and EI index is not simple.

A global warming signal recognized in the observation is highlighted to investigate whether the SST trend due to global warming is closer to that of El Niño or La Niña (Meehl et al. 1996; Sun and Liu 1996; Cane et al. 1997; Seager and Murtugudde 1997; Collins et al. 2005; An 2011). This issue is important because it indicates different global impacts due to global warming; this study also suggests that the spatial pattern of SST trend due to global warming is important for determining the characteristics of El Niño events. However, it should be noted that the conclusion in this study is based on a single global warming scenario, RCP4.5. To obtain a rigorous conclusion, this relationship can be verified by determining whether the changes in climatology and independency between the two types of El Niño events are valid in other warming scenarios.

Acknowledgments. Y.-G. Ham and Y. Jeong were funded by the Korean Meteorological Administration Research and Development Program under Grant KMIPA2015-1040-1. J.-S. Kug was supported by the Korean Meteorological Administration Research and Development Program under Grant KMIPA2015-2092.

REFERENCES

Allen, M. R., and W. J. Ingram, 2002: Constraints on future changes in climate and the hydrologic cycle. *Nature*, **419**, 224–232, doi:10.1038/nature01092.

An, S.-I., 2011: Atmospheric responses of Gill-type and Lindzen–Nigam models to global warming. *J. Climate*, **24**, 6165–6173, doi:10.1175/2011JCLI3971.1.

——, J.-S. Kug, Y.-G. Ham, and I.-S. Kang, 2008: Successive modulation of ENSO to the future greenhouse warming. *J. Climate*, **21**, 3–21, doi:10.1175/2007JCLI1500.1.

——, J.-W. Kim, S.-H. Im, B.-M. Kim, and J.-H. Park, 2012: Recent and future sea surface temperature trends in tropical Pacific warm pool and cold tongue regions. *Climate Dyn.*, **39**, 1373–1383, doi:10.1007/s00382-011-1129-7.

Ashok, K., and T. Yamagata, 2009: Climate change: The El Niño with a difference. *Nature*, **461**, 481–484, doi:10.1038/461481a.

——, S. K. Behera, S. A. Rao, H. Weng, and T. Yamagata, 2007: El Niño Modoki and its possible teleconnection. *J. Geophys. Res.*, **112**, C11007, doi:10.1029/2006JC003798.

Cai, W., and Coauthors, 2014: Increasing frequency of extreme El Niño events due to greenhouse warming. *Nat. Climate Change*, **4**, 111–116, doi:10.1038/nclimate2100.

Cane, M. A., A. C. Clement, A. Kaplan, Y. Kushnir, D. Pozdnyakov, R. Seager, S. E. Zebiak, and R. Murtugudde, 1997: Twentieth-century sea surface temperature trends. *Science*, **275**, 957–960, doi:10.1126/science.275.5302.957.

Chou, C., J. D. Neelin, C. A. Chen, and J. Y. Tu, 2009: Evaluating the "rich-get-richer" mechanism in tropical precipitation change under global warming. *J. Climate*, **22**, 1982–2005, doi:10.1175/2008JCLI2471.1.

Collins, M., and Coauthors, 2005: El Niño- or La Niña-like climate change? *Climate Dyn.*, **24**, 89–104, doi:10.1007/s00382-004-0478-x.

——, and Coauthors, 2010: The impact of global warming on the tropical Pacific Ocean and El Niño. *Nat. Geosci.*, **3**, 391–397, doi:10.1038/ngeo868.

Ham, Y.-G., and J.-S. Kug, 2012: How well do current climate models simulate two types of El Nino? *Climate Dyn.*, **39**, 383–398, doi:10.1007/s00382-011-1157-3.

——, and ——, 2014: Effects of Pacific Intertropical Convergence Zone precipitation bias on ENSO phase transition. *Environ. Res. Lett.*, **9**, 064008, doi:10.1088/1748-9326/9/6/064008.

——, ——, and M.-J. Lim, 2012: Rectification feedback of high-frequency atmospheric variability into low-frequency zonal flows in the tropical Pacific. *J. Climate*, **25**, 5088–5101, doi:10.1175/JCLI-D-11-00303.1.

Held, I. M., and B. J. Soden, 2006: Robust responses of the hydrological cycle to global warming. *J. Climate*, **19**, 5686–5699, doi:10.1175/JCLI3990.1.

IPCC, 2014: *Climate Change 2013: The Physical Science Basis.* Cambridge University Press, 1535 pp.

Jin, F.-F., and S.-I. An, 1999: Thermocline and zonal advective feedbacks within the equatorial ocean recharge oscillator model for ENSO. *Geophys. Res. Lett.*, **26**, 2989–2992, doi:10.1029/1999GL002297.

Johnson, N. C., 2013: How many ENSO flavors can we distinguish? *J. Climate*, **26**, 4816–4827, doi:10.1175/JCLI-D-12-00649.1.

——, 2014: Atmospheric science: A boost in big El Niño. *Nat. Climate Change*, **4**, 90–91, doi:10.1038/nclimate2108.

Kang, I.-S., and J.-S. Kug, 2002: El Niño and La Niña sea surface temperature anomalies: Asymmetry characteristics associated with their wind stress anomalies. *J. Geophys. Res.*, **107**, 4372, doi:10.1029/2001JD000393.

Kao, H.-Y., and J.-Y. Yu, 2009: Contrasting eastern-Pacific and central-Pacific types of ENSO. *J. Climate*, **22**, 615–632, doi:10.1175/2008JCLI2309.1.

Kessler, W. S., and R. Kleeman, 2000: Rectification of the Madden–Julian oscillation into the ENSO cycle. *J. Climate*, **13**, 3560–3575, doi:10.1175/1520-0442(2000)013<3560:ROTMJO>2.0.CO;2.

Kim, D., J.-S. Kug, I.-S. Kang, F.-F. Jin, and A. T. Wittenberg, 2008: Tropical Pacific impacts of convective momentum transport in the SNU coupled GCM. *Climate Dyn.*, **31**, 213–226, doi:10.1007/s00382-007-0348-4.

——, Y.-S. Jang, D.-H. Kim, Y.-H. Kim, M. Watanabe, F.-F. Jin, and J.-S. Kug, 2011: El Niño–Southern Oscillation sensitivity to cumulus entrainment in a coupled general circulation model. *J. Geophys. Res.*, **116**, D22112, doi:10.1029/2011JD016526.

Kug, J.-S., and Y.-G. Ham, 2011: Are there two types of La Nina? *Geophys. Res. Lett.*, **38**, L16704, doi:10.1029/2011GL048237.

——, F.-F. Jin, and S.-I. An, 2009: Two types of El Niño events: Cold tongue El Niño and warm pool El Niño. *J. Climate*, **22**, 1499–1515, doi:10.1175/2008JCLI2624.1.

——, S.-I. An, Y.-G. Ham, and I.-S. Kang, 2010a: Changes in El Niño and La Niña teleconnections over North Pacific–America in the global warming simulation. *Theor. Appl. Climatol.*, **100**, 275–282, doi:10.1007/s00704-009-0183-0.

——, J. Choi, S.-I. An, F.-F. Jin, and A. T. Wittenberg, 2010b: Warm pool and cold tongue El Niño events as simulated by the GFDL 2.1 coupled GCM. *J. Climate*, **23**, 1226–1239, doi:10.1175/2009JCLI3293.1.

——, K. P. Sooraj, F.-F. Jin, Y.-G. Ham, and D. Kim, 2011: A possible mechanism for El Niño–like warming in response to the future greenhouse warming. *J. Climatol.*, **31**, 1567–1572, doi:10.1002/joc.2163.

——, Y.-G. Ham, J.-Y. Lee, and F.-F. Jin, 2012: Improved simulation of two types of El Niño in CMIP5 models. *Environ. Res. Lett.*, **7**, 034002, doi:10.1088/1748-9326/7/3/034002.

Larkin, N. K., and D. Harrison, 2005a: Global seasonal temperature and precipitation anomalies during El Niño autumn and winter. *Geophys. Res. Lett.*, **32**, L16705, doi:10.1029/2005GL022860.

——, and ——, 2005b: On the definition of El Niño and associated seasonal average U.S. weather anomalies. *Geophys. Res. Lett.*, **32**, L13705, doi:10.1029/2005GL022738.

Lee, T., and M. J. McPhaden, 2010: Increasing intensity of El Niño in the central-equatorial Pacific. *Geophys. Res. Lett.*, **37**, L14603, doi:10.1029/2010GL044007.

Lin, J.-L., 2007: The double-ITCZ problem in IPCC AR4 coupled GCMs: Ocean–atmosphere feedback analysis. *J. Climate*, **20**, 4497–4525, doi:10.1175/JCLI4272.1.

Meehl, G. A., W. M. Washington, D. J. Erickson, B. P. Briegleb, and P. J. Jaumann, 1996: Climate change from increased CO_2 and direct and indirect effects of sulfate aerosols. *Geophys. Res. Lett.*, **23**, 3755–3758, doi:10.1029/96GL03478.

Min, S.-K., and Coauthors, 2015: Changes in weather and climate extremes over Korea and possible causes: A review. *Asia-Pac. J. Atmos. Sci.*, **51**, 103–121, doi:10.1007/s13143-015-0066-5.

Newman, M., S. I. Shin, and M. A. Alexander, 2011: Natural variation in ENSO flavors. *Geophys. Res. Lett.*, **38**, L14705, doi:10.1029/2011GL047658.

Philip, S., and G. J. van Oldenborgh, 2006: Shifts in ENSO coupling processes under global warming. *Geophys. Res. Lett.*, **33**, L11704, doi:10.1029/2006GL026196.

Power, S., F. Delage, C. Chung, G. Kociuba, and K. Keay, 2013: Robust twenty-first-century projections of El Niño and related precipitation variability. *Nature*, **502**, 541–545, doi:10.1038/nature12580.

Seager, R., and R. Murtugudde, 1997: Ocean dynamics, thermocline adjustment, and regulation of tropical SST. *J. Climate*, **10**, 521–534, doi:10.1175/1520-0442(1997)010<0521:ODTAAR>2.0.CO;2.

Seiki, A., Y. N. Takayabu, T. Yasuda, N. Sato, C. Takahashi, K. Yoneyama, and R. Shirooka, 2011: Westerly wind bursts and their relationship with ENSO in CMIP3 models. *J. Geophys. Res.*, **116**, D03303, doi:10.1029/2010JD015039.

Smith, T. M., R. W. Reynolds, T. C. Peterson, and J. Lawrimore, 2008: Improvements to NOAA's historical merged land–ocean surface temperature analysis (1880–2006). *J. Climate*, **21**, 2283–2296, doi:10.1175/2007JCLI2100.1.

Spencer, R. W., and W. D. Braswell, 2014: The role of ENSO in global ocean temperature changes during 1955–2011 simulated with a 1D climate model. *Asia-Pac. J. Atmos. Sci.*, **50**, 229–237, doi:10.1007/s13143-014-0011-z.

Sun, D.-Z., and Z. Liu, 1996: Dynamic ocean–atmosphere coupling: A thermostat for the tropics. *Science*, **272**, 1148–1149, doi:10.1126/science.272.5265.1148.

Takahashi, K., A. Montecinos, K. Goubanova, and B. Dewitte, 2011: ENSO regimes: Reinterpreting the canonical and Modoki El Niño. *Geophys. Res. Lett.*, **38**, L10704, doi:10.1029/2011GL047364.

Taschetto, A. S., A. Sen Gupta, N. C. Jourdain, A. Santoso, C. C. Ummenhofer, and M. H. England, 2014: Cold tongue and warm pool ENSO events in CMIP5: Mean state and future projections. *J. Climate*, **27**, 2861–2885, doi:10.1175/JCLI-D-13-00437.1.

van Oldenborgh, G. J., S. Philip, and M. Collins, 2005: El Niño in a changing climate: A multi-model study. *Ocean Sci. Discuss.*, **2**, 267–298, doi:10.5194/osd-2-267-2005.

Vecchi, G. A., and A. T. Wittenberg, 2010: El Niño and our future climate: Where do we stand? *Wiley Interdiscip. Rev.: Climate Change*, **1**, 260–270, doi:10.1002/wcc.33.

——, B. J. Soden, A. T. Wittenberg, I. M. Held, A. Leetmaa, and M. J. Harrison, 2006: Weakening of tropical Pacific atmospheric circulation due to anthropogenic forcing. *Nature*, **441**, 73–76, doi:10.1038/nature04744.

Watanabe, M., and A. T. Wittenberg, 2012: A method for disentangling El Niño–mean state interaction. *Geophys. Res. Lett.*, **39**, L14702, doi:10.1029/2012GL052013.

——, J.-S. Kug, F.-F. Jin, M. Collins, M. Ohba, and A. Wittenberg, 2012: Uncertainty in the ENSO amplitude change from the past to the future. *Geophys. Res. Lett.*, **39**, L20703, doi:10.1029/2012GL053305.

——, Y. Kamae, and M. Kimoto, 2014: Robust increase of the equatorial Pacific rainfall and its variability in a warmed climate. *Geophys. Res. Lett.*, **41**, 3227–3232, doi:10.1002/2014GL059692.

Yeh, S.-W., J.-S. Kug, B. Dewitte, M.-H. Kwon, B. P. Kirtman, and F.-F. Jin, 2009: El Niño in a changing climate. *Nature*, **461**, 511–514, doi:10.1038/nature08316.

——, B. P. Kirtman, J. S. Kug, W. Park, and M. Latif, 2011: Natural variability of the central Pacific El Niño event on multi-centennial timescales. *Geophys. Res. Lett.*, **38**, L02704, doi:10.1029/2010GL045886.

——, J.-S. Kug, and S.-I. An, 2014: Recent progress on two types of El Niño: Observations, dynamics, and future changes. *Asia-Pac. J. Atmos. Sci.*, **50**, 69–81, doi:10.1007/s13143-014-0028-3.